Numerical Investigation of Baffle Spacing in a Shell and Tube Heat Exchanger with Segmental Baffle

Ravi Gugulothu, Narsimhulu Sanke, Farid Ahmed, Naga Sarada Somanchi, and M. T. Naik

Abstract Baffle spacing has a decisive effect on heat transfer and pumping power. The development of baffle spacing significantly dominates the turbulence created inside the shell and tube heat exchanger and heat transfer. The study will focus on the impact of baffle spacing in both global and local thermo-hydraulic characteristics. The shell side flow rate varied from 0.18 to 0.31 kg/s, whereas the tube side flow rate varied from 0.11 to 0.18 kg/s. The fluid was assumed to be incompressible Newtonian fluid. Finite volume method was implemented to predict the thermal and flow behavior inside the heat exchanger. The simulations were carried out under steady-state assumption. The results show that with the decrease in baffle spacing, the amount of heat transfer rate increases. On the contrary, the increase in pressure drop was observed with the increase in baffle spacing.

Nomenclature

STHE	Shell and Tube Heat Exchanger
P	Tube pitch
d	Tube diameter
D	Shell diameter

R. Gugulothu (✉) · N. Sanke
Department of Mechanical Engineering, University College of Engineering, Osmania University, Hyderabad, India
e-mail: ravi.gugulothu@gmail.com

N. Sanke
e-mail: nsanke@osmania.ac.in

F. Ahmed
Department of Nuclear Science and Engineering, Military Institute of Science and Technology, Dhaka, Bangladesh

N. S. Somanchi · M. T. Naik
Department of Mechanical Engineering, JNTUH College of Engineering Hyderabad, Hyderabad, India

S	Baffle spacing
H	Baffle Cut/height
L	Length
PDEs	Partial Differential Equations
Nu	Nusselt number
De	Effective diameter
Re	Reynolds number
TEMA	Tubular Exchanger Manufacturers Association

Greek symbols

ΔP	Pressure drop (Pa)
U	Overall Heat Transfer Coefficient (W/m^{2}K)

Subscripts

| *s*	Shell
t	Tube
0	Outer
i	Inner
avg	Average

1   Introduction

Heat exchanger devices are used to transfer heat between two or more fluids which are at different temperatures and pressures, separated by a solid wall [1]. In heat exchanger apparatus, shell and tube heat exchanger (STHE) is playing key role (energy generation, oil refining industries, waste to heat recovery systems, etc.) due to robust construction of geometrical structure, ease of upgrade, and maintenance [2, 3]. To calculate the performance of STHE, baffle geometry and arrangement are essential components which are indicated in Fig. 1. Segmental baffle STHE is a commonly used one, and it will lead the fluid flow in tortuous and zigzag manner in the shell body [4–6]. These baffles are improving level of mixing to enhance the heat transfer of STHE which is given in Figs. 1 and 2.

Ramananda Rao et al. [7] studied the shell and tube heat exchanger by choosing the parameters toward minimizing the cost of heat exchanger for any heat duty, author considered tube pitch (P_t) should be 1.25–1.5d$_0$, minimum tube sheet thickness is 3.2 mm, length to diameter ratio should be 3 to 15 and baffle spacing should be 20% of
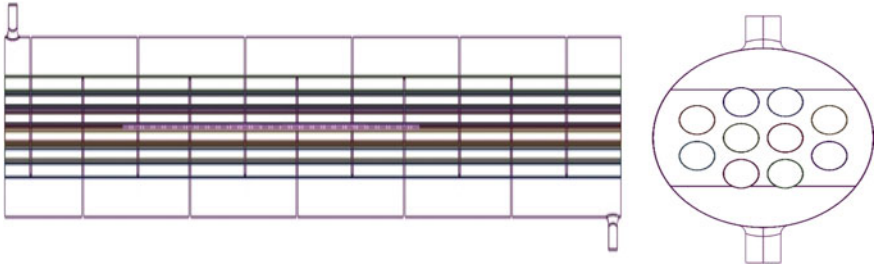
Fig. 1 Segmental baffle shell and tube heat exchanger
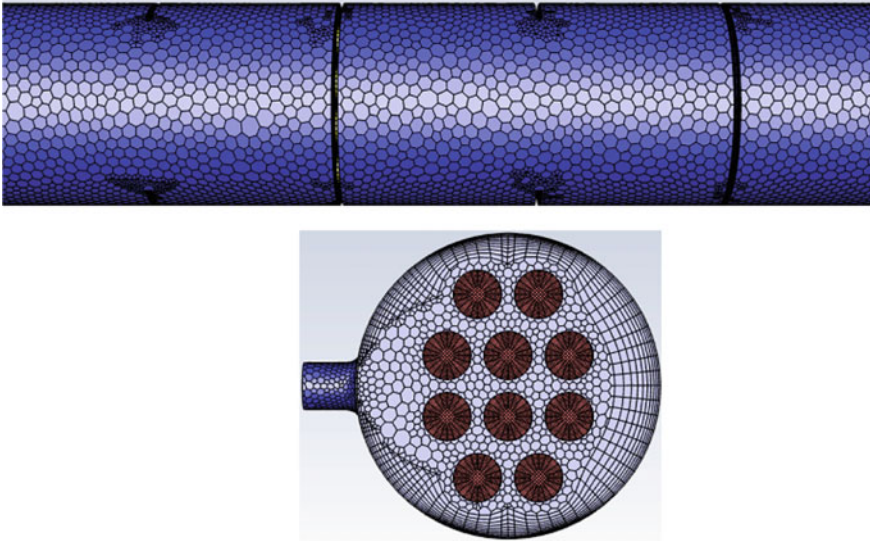
Fig. 2 Mesh geometry

D_i to 100% of D_i, it should not be less than 50 mm and finally concluded that these design parameters shown limited pressure drop and space and length constraints. Khalifeh Soltan et al. [8] listed out 20 and 100%D_i. Saffar Avval et al. [9] presented an optimization program to calculate an optimum baffle spacing and the number of sealing strips for STHE, all most negligible effect found on the optimum pumping power and heat transfer, while the baffle spacing has a noticeable effect by author.

Gaddis et al. [10] presented a procedure to evaluate shell side pressure drop in segmental baffle shell and tube heat exchanger. Author varied the ratio of baffle spacing to shell inside diameter (S/D_i) and the ratio of baffle cut to shell inside diameter (H/D_i) within the range and concluded that $0.2 \leq \left(\frac{S}{D_i}\right) \leq 1$ and $0.15 \leq \left(\frac{H}{D_i}\right) \leq 0.4$. Iyer et al. [11] successfully established and designed optimal STHE. Kallannavar et al. [12] experimentally studied that STHE with different tube

layout as 30^0, 45^0, and 60^0. Among these three tube layouts, 30^0 degree tube layout proved better heat transfer rate. Emad et al. [13] experimentally studied STHE with four different segmental baffle (conventional single segmental baffle, staggered single segmental baffle, flower segmental baffle, and hybrid segmental baffle) configurations to enhance the thermal, hydraulic, and thermodynamic performances. Hybrid segmental baffle configuration STHE is the best among the studied STHE. Gugulothu et al. [14] numerically studied different hydrodynamic characteristics and local parameters of a 3D geometry of shell and tube heat exchangers with segmental baffle.

The objective of the study is to investigate the heat transfer rate of different configured baffled spacing and provide the potential configuration through optimization study. For the investigation, the baffle spacing varied from 50 to 100 mm. The shell side flow rate varied from 0.18 to 0.31 kg/s, whereas the tube side flow rate varied from 0.11 to 0.18 kg/s. The study will put a remark to choose the best configuration of baffle spacing and flow rate considering both the variation of heat transfer rate and pressure drop.

2 Simulation and Modeling

2.1 Governing Equations

In the present investigation, the heat transfer and fluid flow phenomena on the shell side and tube side are studied in shell and tube heat exchanger with segmental baffle. The conservation equation, continuity, momentum, and energy are presented here.

Continuity equation:

$$\frac{\partial(\rho f_v)}{\partial t} + \frac{\partial\left(\rho f_s u_j\right)}{\partial x_j} = 0 \tag{1}$$

Momentum equation:

$$\frac{\partial(\rho f_v u_i)}{\partial t} + \frac{\partial\left(\rho f_s u_i u_j\right)}{\partial x_j} = -f_s \frac{\partial p_i}{\partial x_i} + \frac{\partial\left(f_s \mu_{\text{eff}}\left(\frac{\partial u_i}{\partial x_j} + \frac{\partial u_j}{\partial x_i}\right)\right)}{\partial x_j} - 0.5 f_i \rho |u_i| u_i \tag{2}$$

Energy equation:

$$\frac{\partial\left(\rho c_p f_v T\right)}{\partial t} + \frac{\partial\left(\rho c_p T f_s u_j\right)}{\partial x_j} = \frac{\partial\left(f_s \lambda_{\text{eff}}\left(\frac{\partial T}{\partial x_j}\right)\right)}{\partial x_j} + \Omega K (T_t - T) \tag{3}$$

where u is velocity

2.2 Computational Domain

The STHE as shown in Fig. 1 is a single shell and tube pass with four tubes. The geometry of STHE is shell inner diameter (D_i)=100 mm, length (Ls)=1150 mm, and tube bundle consists with ten tubes of 19 mm outer diameter in triangular arrangement with 25-mm tube pitch.

2.3 Boundary Conditions

The shell and tube heat exchanger consists of two loops carrying the coolant. The cold fluid flows in the shell with a temperature of 303.15 K. The hot fluid flows in four tubes at a temperature of 338.15 K. Several assumptions are made to simplify the geometry and study the numerical computational domain. Those are insulated shell walls, neglected fluid flow leakage, and fully developed fluid flow.

2.4 Mesh Selection and Sensitivity Analysis

STHX is a complex structure, so unstructured tetra-hydrate mesh was selected which is a proper grid system to mesh numerical models, i.e., shown in Fig. 2. Very fine mesh is done nearby tube wall region to obtain more accurate results. The finite volume method with SIMPLE pressure velocity coupling algorithm is used to solve the PDEs. PRESTO method with double precision solver was implemented to solve the convective terms in the governing equations [15–17].

2.5 Data Reduction

Tube outer diameter (d_0) is 16 mm taken,

$$\text{Shell side Nusselt number Nu}_s = 1.86\text{Re}_s^{0.33}\,\underset{s}{\text{Pr}}^{0.33}\left(\frac{D_i}{L}\right)^{0.33} \qquad (4)$$

$$\text{Shell side Reynolds number Re}_s = \frac{D_e V_s}{\vartheta_s} \qquad (5)$$

$$\text{Effective diameter (m) } D_e = \frac{P_t^2 - \frac{\pi d_0^2}{4}}{\frac{\pi d_0}{4}} \tag{6}$$

$$\text{According to TEMA standards } P_t = 1.25d_0 \text{ in mm} \tag{7}$$

$$\text{Shell side Prandtl number } Pr_s = \frac{\mu_s C_{p_s}}{k_s} \tag{8}$$

$$\text{Free flow area } A_s = \frac{\pi}{4}\left(D_i^2 - N_t d_0^2\right) \tag{9}$$

$$\text{Number of tubes } N_t = K_1\left(\frac{D_s}{d_0}\right)^{n_1} \tag{10}$$

No. of passes	Triangular pitch		Square and rotated square pitch	
	K_1	N_1	K_1	n_1
1	0.319	2.142	0.215	2.207
2	0.249	2.207	0.156	2.291
4	0.175	2.285	0.158	2.263
6	0.0743	2.499	0.0402	2.617
8	0.0365	2.675	0.0331	2.643

$$\text{Shell outer diameter } D_s = \frac{D_{\text{otl}}}{0.95} + \delta_{\text{clearence}} \tag{11}$$

$$\text{Tube bundle outer diameter } D_{\text{otl}} = \left(\frac{N_t}{K_1}\right)^{\frac{1}{n_1}} d_0 \tag{12}$$

According to Ravi et al., baffle space (BS) is 20–100%D_i and it should not be less than 51 mm. In this research paper, geometry is created with different baffle spacing from 0.2 to 1D_i and simulation is conducted.

$$\text{Heat exchanger surface area(m}^2) A_0 = \pi N_t d_0 L \tag{13}$$

$$\text{Shell side Nusselt number } \mathrm{Nu}_s = 1.86\mathrm{Re}_s^{0.33} Pr_s^{0.33}\left(\frac{D_i}{L}\right)^{0.33} \tag{14}$$

$$\text{Tube side Reynolds number } \mathrm{Re}_t = \frac{d_i V_t}{\vartheta_t} \tag{15}$$

$$Tube side Prandtl number \ Pr_t = \frac{\mu_t C_{p_t}}{k_t} \tag{16}$$

3 Results and Discussions

3.1 Validation of Results

In order to validate the numerical model, the results of the present study were compared with the experimental study of Kamel et al. [18] following the same boundary conditions. The results of the comparison study are shown in Fig. 3. It is well recognized from the figure that the present study aligns precisely with a good agreement along with the study of Kamel et al. [18]. The maximum errors encountered during the simulation are found to be 14.6% at 0.18 kg/s flow rate, whereas the minimum error of 6.5% was encountered at 0.11 kg/s flow rate. Hence, following the results of the assessment, it could be said that the present numerical model could capture the thermo-hydraulic characteristics of the computational geometry accurately.
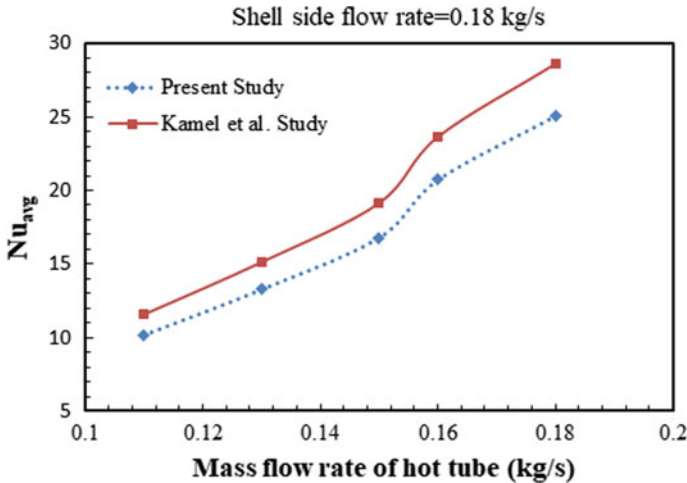

Fig. 3 Comparison of the present study with experimental investigations

3.2 Pressure Drop

The pressure distribution of heat exchangers can reflect the resistance characteristic and heat transfer performance. Figure 4 presents the pressure contour with superimposed fluid velocity. It is well recognized from the figure that along with the flow direction, the pressure drops linearly.

Figure 5 shows the temperature distribution of all the studied six baffle space shell and tube heat exchangers with the segmental baffle. The temperature distribution is shallow behind the baffles, and local heat transfer is very poor. In Fig. 5, tube side temperature will gradually decrease from 338.15 to 322.618 K by increasing the
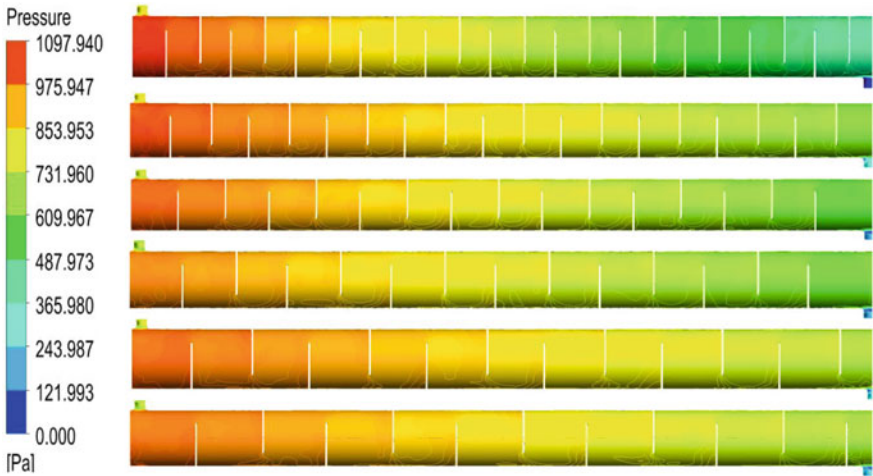

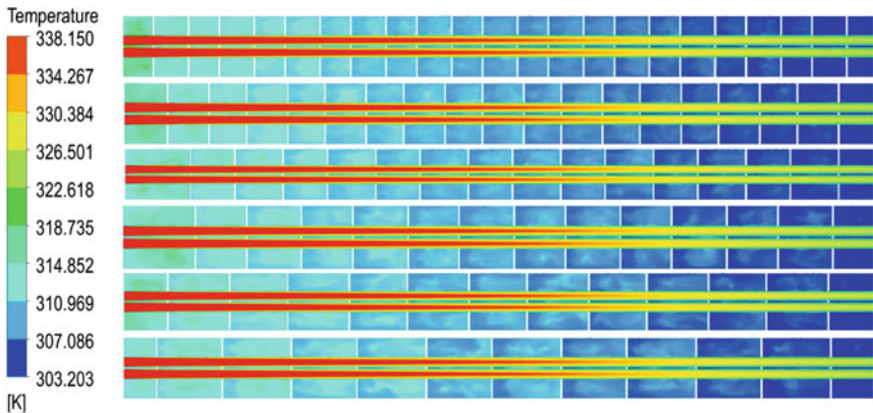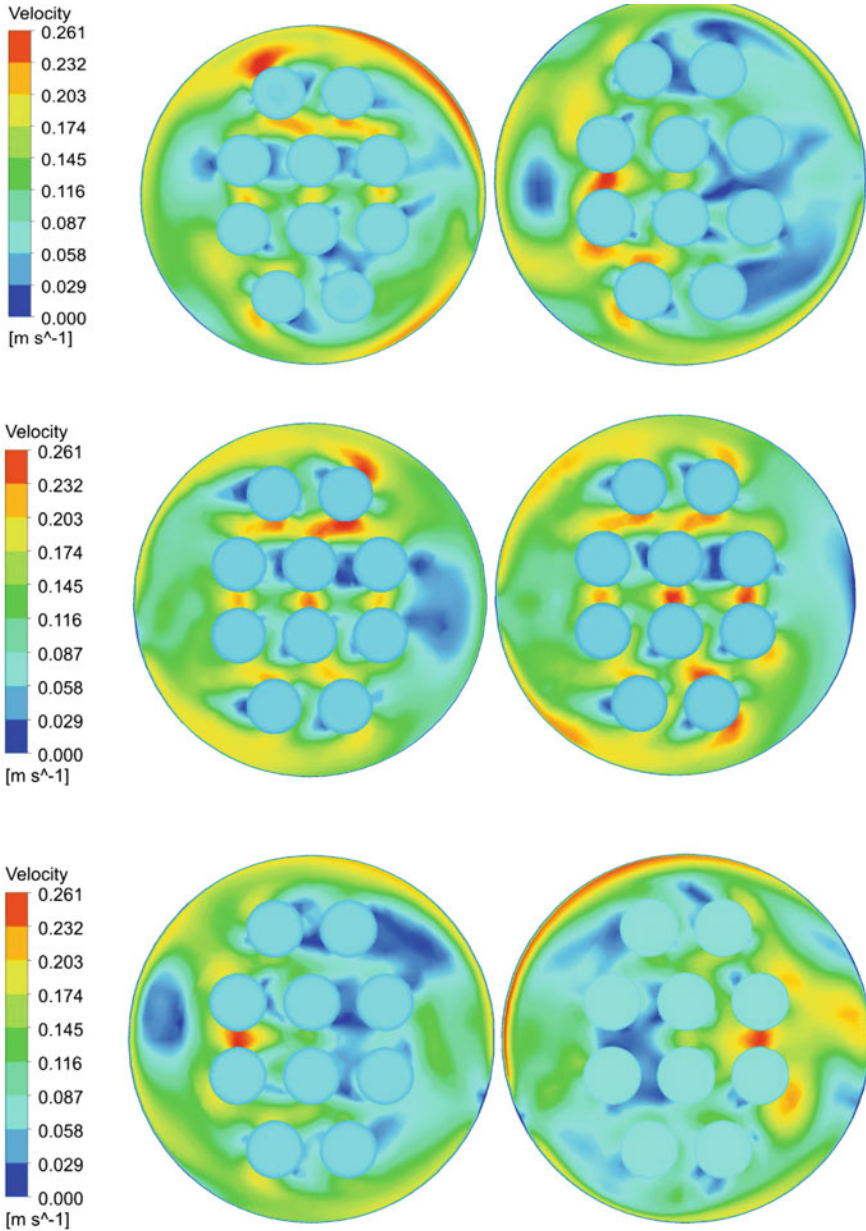**Fig. 4** Shell side pressure of $m_s = 0.18$ kg/s and $m_t = 0.11$ to 0.18 kg/s

Fig. 5 Temperature in x–y plane of $m_s = 0.18$ kg/s and $m_t = 0.11$ to 0.18 kg/s

shell side temperature until 314 K. It is noticed that the temperature is higher and gradually reduces near the shell wall center.

The velocity contours of computational flow domain are shown in Fig. 6 for

Fig. 6 Velocity at $x = 0.24$ m of radial plane of $m_s = 0.18$ kg/s and $m_t = 0.11$ to 0.18 kg/s

the radial velocity at $x=0.24$ m distance. These contours are demonstrated in radial directions, and the authors noticed that due to the presence of the baffles, the vortex formations is observed which initiates the secondary flow in the flow regime. Such phenomenon of inducing secondary flow with the help of initiating and increasing turbulent intensity improves the heat transfer rate of the flow domain. Due to having lower space within the baffles, 50-mm baffle spacing induces higher secondary flow, which gradually decreases with the increase in baffle spacing and the least amount of secondary flow is evaluated for 100-mm baffle spacing. Consequently, it is recognized that 50-mm baffle spacing improves the heat transfer rate most, which gradually decreases with the increase in baffle spacing and least amount of improvement is observed for 100-mm baffle spacing. In addition, the upsurge in velocity gradient near the walls of the computational geometry is evident since the leakage zones in the heat exchanger decreases the velocity at shell center and increases at shell walls.

Figure 7 represents the average heat transfer and fluid flow characteristics across tube bundles in shell body at different baffle space from 50 to 100 mm. According
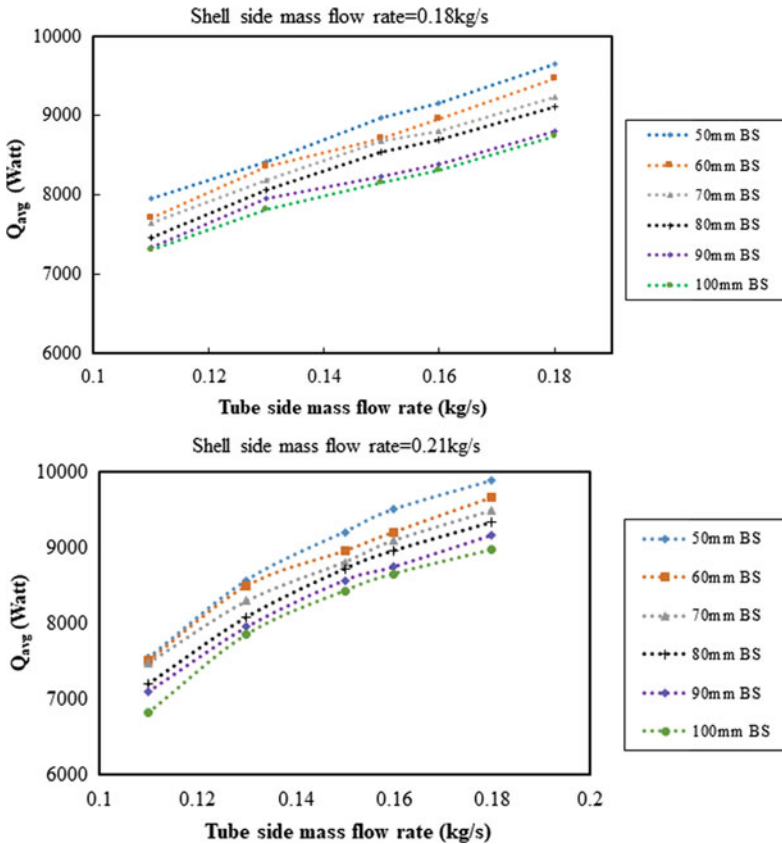

Fig. 7 Average heat transfer rate of $m_s = 0.18$ kg/s and $m_t = 0.11$ kg/s
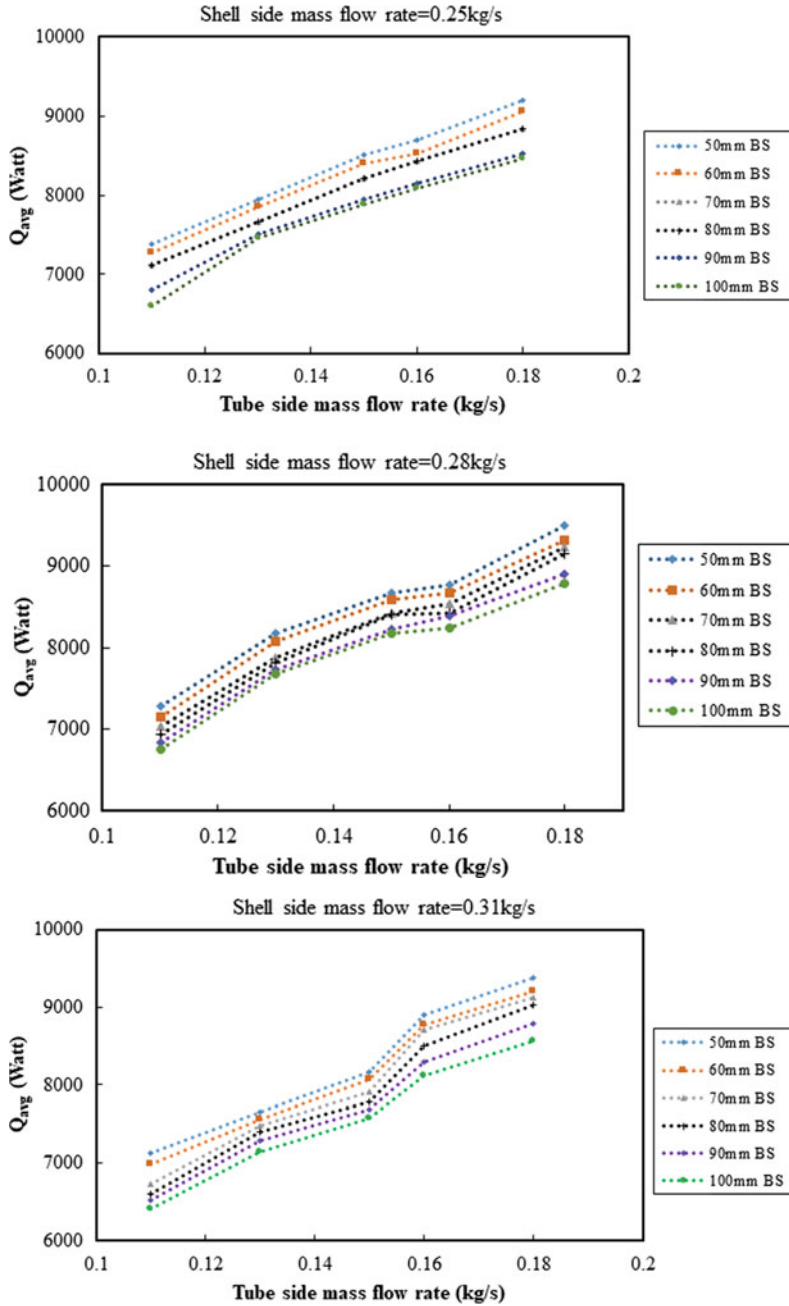
Fig. 7 (continued)

to Fig. 7, heat transfer rate is increasing along with the increase in mass flow rate and baffle spacing. The fluctuation of the flow pattern increases with the decrease in baffle spacing, which eventually increases the turbulent intensity. Since the turbulent intensity plays as a predominant parameter in enhancement of heat transfer, lowering the baffle spacing induces higher heat transfer rate. As a result, the highest heat transfer rate was observed at 50-mm baffle spacing in Fig. 7, which progressively decreases with the increase in baffle spacing and achieved lowest value of heat transfer rate at 100-mm baffle spacing.

Figure 8 indicates the pressure drop of all the studied shell and tube heat exchanger with different baffle spaces from 50 to 100 mm, i.e., 20–1%D_i. From Fig. 8, it is identified that with the decrease in baffle spacing, the pressure drop increases. The maximum pressure drop was observed for 50-mm baffle spacing, which gradually decreases with the increase in baffle spacing, and lowest value of pressure drop was recognized for 100-mm baffle spacing.

4   Conclusion

In this research paper, work is done with different baffle space from 20 to 100%D_i with segmental baffle shell and tube heat exchanger. In this work, 20%D_i baffle space showed more pressure, high heat transfer, and 100%D_i baffle space shown as less pressure and less heat transfer. Moreover, 70- and 80-mm baffle spacing in segmental baffle has shown the optimal solutions. The study will privilege the heat exchanger industries to implement the optimized configuration of baffle spacing, taking both heat transfer and pressure drop into consideration.
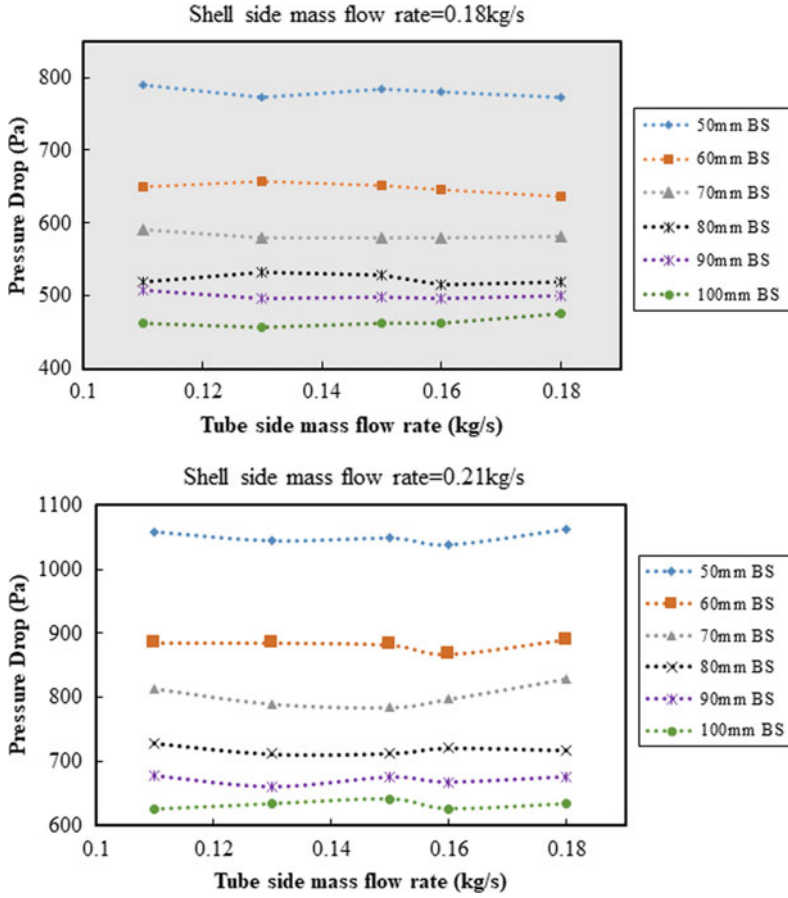
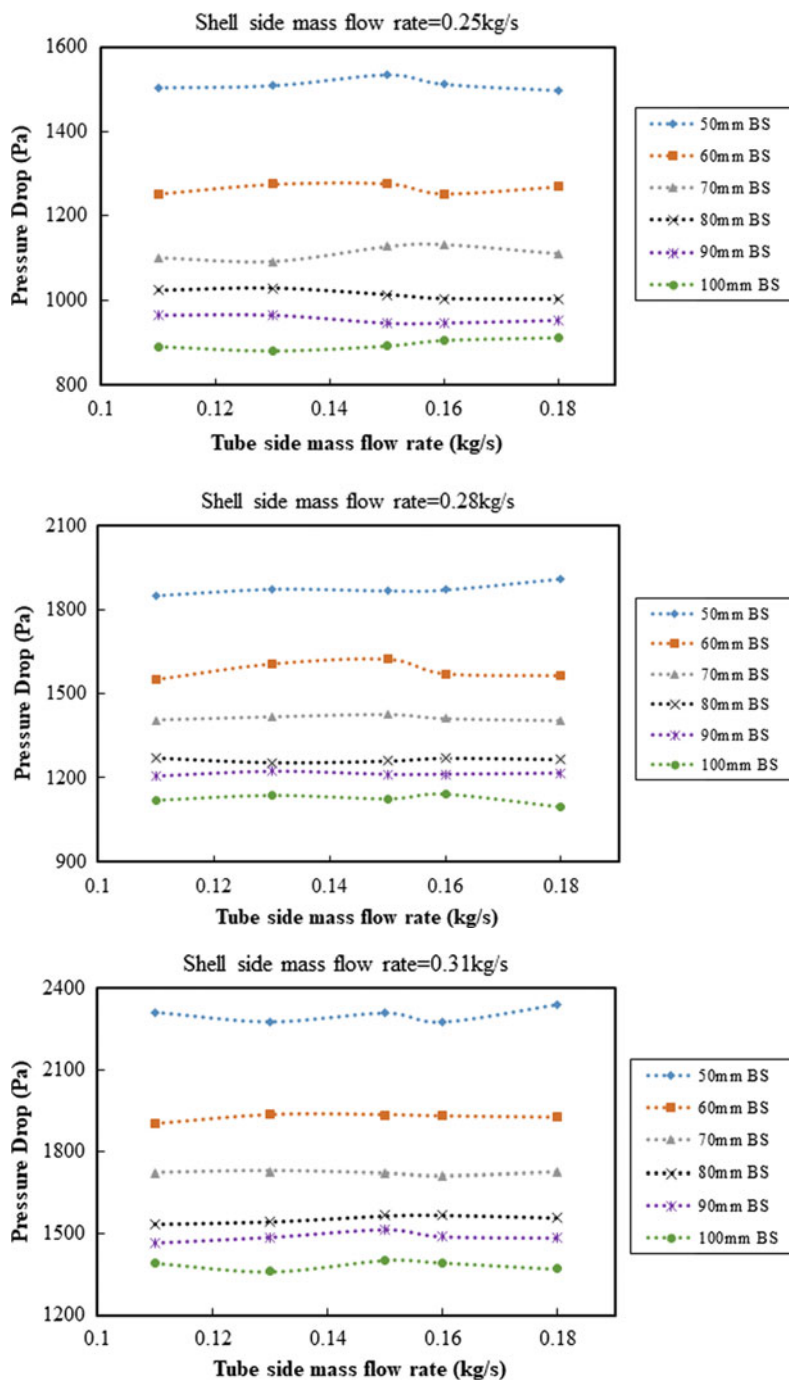Fig. 8 Pressure drop of $m_s = 0.18$ kg/s and $m_t = 0.11$ kg/s

Fig. 8 (continued)

References

1. Hadidi A, Hadidi M, Nazari A (2013) A new design approach for shell and tube heat exchangers using imperialist competitive algorithm (IAC) from economic point of view. Energy Convers Manage 67(2013):66–74

2. Gugulothu R, Somanchi NS, Reddy VK, Tirkey JV (2016) A review on design of baffles for shell and tube heat exchangers. In: Proceeding of ACGT-2016, Indian Institute of Technology Bombay, during 14–16th Nov 2016

3. Gugulothu R, Sanke N, Gupta AVSSKS (2018) Numerical study of heat transfer characteristics in shell and tube heat exchanger. In: Lecture notes in mechanical engineering. Springer Nature Singapore Pte Ltd. 2019, pp 375–383

4. Gugulothu R, Vijaya Kumar Reddy K, Somanchi NS, Adithya EL (2017) A review on enhancement of heat transfer techniques. In: 5th international conference of materials processing and characterization (ICMPC-2016), Materials Today: Proceedings, vol 4, pp 1051–1056

5. Vijaya Kumar Reddy K, Sudheer Prem Kumar B, Gugulothu R, Anuja K, Vijaya Rao P (2017) CFD analysis of a helically coiled tube in tube heat exchanger. In: 5th international conference of materials processing and characterization (ICMPC-2016), materials today: proceedings, vol 4, pp 2341–2349

6. Gugulothu R, Sanke N, Ahmed F, Jilugu RK (2020) Numerical study on shell and tube heat exchanger with segmental baffle. In: International joint conference on advances in computational intelligence (IJCACI-2020), at Daffodil International University Dhaka, Bangladesh, during 20–21st Nov 2020

7. Ramananda Rao R, Shrinivasa U, Srinivasan J (1991) Synthesis of cost optimal shell and tube heat exchangers. Heat Transfer Eng 12(3):47–55

8. Khalifeh Soltan B, Saffar Avval M, Damangir E (2004) Short communication: minimizing capital and operating costs of shell and tube condensers using optimum baffle spacing. Appl Therm Eng 24(2004):2801–2810

9. Saffar Avval M, Damangir E (1995) A general correlation for determining optimum baffle spacing for all types of shell and tube exchangers. Int J Heat Mass Transfer 38(13):2501–2506

10. Gaddis ES, Gnielinski V (1997) Pressure drop on the shell side of shell and tube heat exchangers with segmental baffles. Chem Eng Process 36:149–159

11. Iyer VH, Mahesh S, Malpani R, Sapre M, Kulkarni AJ (2019) Adaptive range genetic algorithm: a hybrid optimization approach and its application in the design and economic optimization of shell and tube heat exchanger. Eng Appl Artif Intell 85:444–461

12. Kallannavar S, Mashyal S, Rajangale M (2019) Effect of tube layout on the performance of shell and tube heat exchangers. In: Mater Today: Proc

13. El Said EMS, Abou Al Sood MM (2019) Shell and tube heat exchanger with new segmental baffles configurations: a comparative experimental investigation. Appl Therm Eng 150:803–810

14. Gugulothu R, Sanke N, Ahmed F, Jilugu RK (2021) Numerical study on shell and tube heat exchanger with segmental baffle. In: Proceedings of international joint conference on advances in computational intelligence, algorithms for intelligent systems. Springer Nature Singapore Pte. Ltd. pp 309–318

15. Ahmed F, Abir MA, Bhowmik PK, Deshpande V, Mollah AS, Kumar D, Alam S (2021) Computational assessment of thermo-hydraulic performance of Al_2O_3 water nanofluid in hexagonal rod-bundles subchannel. Prog Nuclear Energy 135:103700

16. Ahmed F, Abir Md A, Fuad M, Akter F, Bhowmik PK, Alam S, Kumar D (2021) Numerical investigation of the thermo hydraulic performance of water based nanofluids in a dimpled channel flow using Al_2O_3, CuO and hybrid Al_2O_3-CuO as nanoparticles. In: Heat transfer, pp 1–26

17. Fluent ANSYS (2015) Ansys fluent. Academic Research. Release, 14

18. Shirvan KM, Mamourian M, Esfahabi JA (2018) Experimental investigation on thermal performance and economic analysis of cosine wave tube structure in a shell and tube heat exchanger. Energy Conver Manag 175:86–98

19. Yang JF, Zeng M, Wang QW (2015) Numerical investigation on shell side performances of combined parallel and serial two shell pass shell and tube heat exchangers with continuous helical baffles. Appl Energy 139:163–174

20. Gugulothu R, Sanke N (2022) Use of segmental baffle in shell and tube heat exchanger for nano emulsions. Heat Trans 51(3):2645–2666. https://doi.org/10.1002/htj.22418

21. Gugulothu R, Sanke N (2022) Effect of helical baffles and water-based Al_2O_3, CuO, and SiO_2 nanoparticles in the enhancement of thermal performance for shell and tube heat exchanger. Heat Trans. https://doi.org/10.1002/htj.22474